SPECKLE AND INTENSITY INTERFEROMETRY. APPLICATIONS TO ASTRONOMY

F. RODDIER - Université de Nice

I/ - STATISTICAL PROPERTIES OF THERMAL RADIATIONS

We shall mainly deal with the wave aspect of thermal radiations. A thermal radiation is classicaly considered as a random electromagnetic field. When dealing with steady sources, the field is described as a *stationary random process*. Thermal emission is incoherent, i.e. radiations emitted by individual atoms are statistically independant. The resulting field, being the sum of a large number of statistically independant processes, is therefore a *Gaussian process*, as a consequence of the central-limit theorem. A Gaussian process is a process which has Gaussian probability density functions (p.d.f.), i.e. the joint probability density function of the field at any number of points at any time is given by a multidimensional Gaussian law.

We shall only deal with quasimonochromatic fields for which the field bandwidth $\Delta\omega$ is much smaller that the average frequency ω . Using scalar theory, such a field can be expressed, in complex notation, as

$$Z(\vec{r},t) = \psi(\vec{r},t) \exp - i\omega t \qquad (1)$$

where $\vec{r}$ and t are space and time coordinates. ψ is a generalised complex amplitude with negligible variations during the period $2\pi/\omega$. ψ is often refered to as the analytic signal. It is a circular complex Gaussian process, i.e. the variance of the real part is equal to the variance of the imaginary part.

A Gaussian process is entirely defined by its first and second order moment. The first order moment $\langle\psi(\vec{r},t)\rangle$ is zero for a circular process . Since our process is stationary, the second order moment $\langle\psi(\vec{r}_1,t_1)\psi^*(\vec{r}_2,t_2)\rangle$ is a function $C(\Delta\vec{r},\Delta t)$ of the spacing $\Delta\vec{r}$ and of the time delay $\Delta\vec{t}$. It goes to zero when the time delay Δt is much larger than the correlation time τ , which is of the order of $1/\Delta\omega$.

Since there is a finite correlation time τ , our process is also ergodic. This means that a time average taken over a time interval, T , much larger than τ , can be considered as an ensemble average.

In the following, we shall be interested only in the spatial properties of the process $\psi(\vec{r},t)$, that is we shall only consider time delays Δt small compared with the correlation time τ, and we shall examine the properties of the spatial covariance $\langle\psi_1\psi_2^{\star}\rangle$ where ψ_1 and ψ_2 denote $\psi(\vec{r}_1)$ and $\psi(\vec{r}_2)$.

II/ - SPATIAL COHERENCE AND ZERNIKE'S THEOREM

Let us consider the fundamental Young's holes experiment (figure below). In this experiment a thermal light source illuminates a mask with two pinholes. Let ψ_1 and ψ_2 be the complex amplitudes of the field at each hole. Behind the mask, the two holes behave like point sources, and at some distance from the mask, near the axis of symmetry, the complex amplitude is proportional to

$$\psi = \psi_1 + \psi_2 \exp i\phi \qquad (2)$$

where ϕ is the phase difference due to the inequality in the optical path length between the two illuminating beams.

The observed illumination, given by the squared modulus of the field amplitude, is therefore proportional to

$$I = \langle|\psi|^2\rangle = \langle|\psi_1+\psi_2 \exp i\phi|^2\rangle \qquad (3)$$

where the time integration of the eye, made over a time interval much larger than the correlation time τ , has been replaced by an ensemble average

Expanding equation (3) leads to

$$I = \langle|\psi_1|^2 + \langle|\psi_2|^2\rangle + 2\mathrm{Re}\,\langle\psi_1\psi_2^{\star}\rangle \exp -i\phi \qquad (4)$$

in which the complex covariance, $\langle\psi_1\psi_2^{\star}\rangle$, appears. Let θ be the phase of this complex quantity, so that

$$\langle\psi_1\psi_2^{\star}\rangle = \left|\langle\psi_1\psi_2^{\star}\rangle\right| \exp i\theta \qquad (5)$$

and let us suppose that

$$\langle|\psi_1|^2\rangle = \langle|\psi_2|^2\rangle = \sqrt{\langle\psi_1^2\rangle\langle\psi_2^2\rangle} \qquad (6)$$

i.e. the irradiance output from each hole is equal. Equation (4) becomes

$$I = 2\left[\sqrt{\langle\psi_1^2\rangle\langle\psi_2^2\rangle} + |\langle\psi_1\psi_2^{\star}\rangle| \cos(\theta-\phi)\right] \qquad (7)$$

The cosine term of equation (7) describes Young fringes. Let I max and Imin be the associated maxima and minima of I . The fringe visibility is given by the symmetrized expression

$$V = \frac{I\text{max} - I\text{min}}{I\text{max} + I\text{min}} = \frac{|\langle\psi_1\psi_2^{\star}\rangle|}{\sqrt{\langle|\psi_1|^2\rangle\langle|\psi_2|^2\rangle}} = |\Gamma| \qquad (8)$$

where Γ is the normalized complex covariance. $|\Gamma|$ is called the degree of coherence between ψ_1 and ψ_2 .

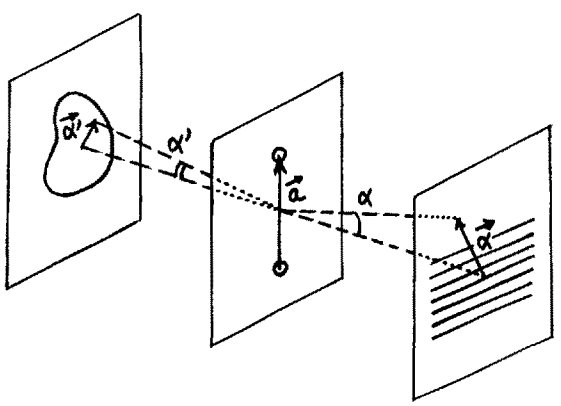

Young's hole experiment

Let us consider a point source illuminating the mask from a direction $\vec{\alpha}'$ (see figure) and let $J(\vec{\alpha}')$ be the irradiance output of each hole, produced by the spherical wave issuing from that point source. At the hole entrance the complex amplitudes are identical, but one is delayed with respect to the other, so that

$$\begin{aligned} &\langle|\psi_1|^2\rangle = \langle|\psi_2|^2\rangle = J(\vec{\alpha}') \\ \text{and} \quad &\langle\psi_1\psi_2^{\star}\rangle = J(\vec{\alpha}') \exp - i\phi' \end{aligned} \tag{9}$$

The illumination in the observed fringe pattern in a direction $\vec{\alpha}$ (see figure) is given by equation (7) which leads to

$$I_o(\vec{\alpha},\vec{\alpha}') = 2J(\vec{\alpha}')\left[1+ \cos -(\phi+\phi')\right] \tag{10}$$

In the paraxial approximation,

$$\phi = \frac{2\pi}{\lambda}\vec{a}.\vec{\alpha} \qquad \text{and} \qquad \phi' = \frac{2\pi}{\lambda}\vec{a}.\vec{\alpha}' \tag{11}$$

where $\vec{a}$ is the position vector of hole 1 with respect to hole 2 (see figure), and equation (10) becomes

$$I_o(\vec{\alpha},\vec{\alpha}') = 2J(\vec{\alpha}')\left[1 + \cos - \frac{2\pi}{\lambda}\vec{a}(\vec{\alpha} + \vec{\alpha}')\right] \tag{12}$$

In this case, the fringe visibility equals 1, since the degree of coherence between ψ_1 and ψ_2 is also unity.

Let us now consider an extended, spatially incoherent source. Each point of the source will produce a fringe pattern described by equation (12) and - since the source is incoherent - all the fringe patterns will add in intensity so that the resulting illumination will be proportional to

$$\begin{aligned} I(\vec{\alpha}) &= \int I_o(\vec{\alpha},\vec{\alpha}')d\vec{\alpha}' \\ &= 2\int J(\vec{\alpha}')d\vec{\alpha}' + 2\int J(\vec{\alpha}') \cos - \frac{2\pi}{\lambda}\vec{a}(\vec{\alpha} + \vec{\alpha}').d\vec{\alpha}' \\ &= 2\int J(\vec{\alpha}')d\vec{\alpha}' + 2\mathrm{Re} \exp - \frac{2i\pi}{\lambda}\vec{a}\vec{\alpha}\int J(\vec{\alpha}')\exp - \frac{2i\pi}{\lambda}\vec{a}\vec{\alpha}'.d\vec{\alpha}' \end{aligned}$$

$$= 2\hat{J}(0) + 2\mathrm{Re}\ \exp - \frac{2i\pi}{\lambda}\vec{\alpha}\vec{\alpha}\ \hat{J}(\frac{\vec{\alpha}}{\lambda})$$

$$= 2\left[\hat{J}(0) + \left|\hat{J}(\frac{\vec{\alpha}}{\lambda})\right|\cos\ (\theta - \frac{2\pi\vec{\alpha}\vec{\alpha}}{\lambda})\right] \qquad (13)$$

where $\hat{J}$ is the Fourier transform of J and θ is the phase of this Fourier transform.

A comparison between (13) and the general expression (7) shows that

$$\Gamma = \frac{<\psi_1\psi_2^{\star}>}{\sqrt{<|\psi_1|^2><|\psi_2|^2>}} = \frac{\hat{J}(\vec{\alpha}/\lambda)}{\hat{J}(0)} \qquad (14)$$

The normalized covariance Γ between ψ_1 and ψ_2, also called complex degree of coherence, is given by the Fourier transform of the intensity distribution in the extended incoherent source, normalized to unity at the origin. (Zernike's theorem).

III/- FOURTH ORDER STATISTICS AND INTENSITY INTERFEROMETRY

Let us now consider the statistical properties of the instantaneous intensity $|\psi(\vec{r},t)|^2$. They can be entirely deduced from the statistics of $\psi(r,t)$. Since ψ is a complex circular Gaussian process, the one-dimensional probability density function of $|\psi|$ is a Rayleigh density and the one-dimensional p.d.f. of $|\psi|^2$ is an exponential density (such statistics occur in any two-dimensional random walk process). This means that the instantaneous intensity $|\psi|^2$ undergoes large fluctuations with a high probability of complete extinction (the exponential distribution is infinite at the origin).

It can be shown that the correlation time of the intensity fluctuations is of the order of the correlation time τ of the fluctuations of ψ that is of the order of the inverse of the bandwidth $\Delta\omega$.

We shall rather focus our attention on the spatial correlation scale of the intensity fluctuations and show that it is also of the order of the correlation scale of ψ.

Let

$$\Delta I = |\psi|^2 - <|\psi|^2> \qquad (15)$$

be the intensity fluctuation and let us calculate the spatial covariance

$$\langle \Delta I_1 . \Delta I_2 \rangle = \langle |\psi_1|^2 |\psi_2|^2 \rangle - \langle |\psi_1|^2 \rangle \langle |\psi_2|^2 \rangle \tag{16}$$

between the intensity fluctuations ΔI_1 and ΔI_2 at two points $\vec{r}_1$ and $\vec{r}_2$

Since ψ is a Gaussian process any fourth order moment can be expressed as a function of the second order moment. In the complex case the relation is

$$\langle \psi_1 \psi_2^{\star} \psi_3 \psi_4^{\star} \rangle = \langle \psi_1 \psi_2^{\star} \rangle \langle \psi_3 \psi_4^{\star} \rangle + \langle \psi_1 \psi_4^{\star} \rangle \langle \psi_2^{\star} \psi_3 \rangle \tag{17}$$

so that

$$\begin{aligned} \langle |\psi_1|^2 |\psi_2|^2 \rangle &= \langle \psi_1 \psi_1^{\star} \psi_2 \psi_2^{\star} \rangle \\ &= \langle \psi_1 \psi_1^{\star} \rangle \langle \psi_2 \psi_2^{\star} \rangle + \langle \psi_1 \psi_2^{\star} \rangle \langle \psi_1^{\star} \psi_2 \rangle \\ &= \langle |\psi_1|^2 \rangle \cdot \langle |\psi_2|^2 \rangle + |\langle \psi_1 \psi_2^{\star} \rangle|^2 \end{aligned} \tag{18}$$

Putting (18) into (16) leads to

$$\langle \Delta I_1 \, \Delta I_2 \rangle = |\langle \psi_1 \psi_2^{\star} \rangle|^2 \tag{19}$$

showing that the covariance of the intensity fluctuations is the squared modulus of the covariance of the complex amplitude. The correlation scale of the intensity fluctuations is therefore of the order of the correlation scale of ψ .

Applying equation (19) to the same point, $\vec{r}_1 = \vec{r}_2 = \vec{r}$ leads to

$$\langle (\Delta I)^2 \rangle = |\langle |\psi|^2 \rangle|^2 = \langle I \rangle^2 \tag{20}$$

showing that the standard deviation $\sqrt{\langle (\Delta I)^2 \rangle}$ of the intensity fluctuations is equal to the average intensity $\langle I \rangle$.

Normalizing equation (19) leads to

$$\frac{\langle \Delta I_1 \, \Delta I_2 \rangle}{\sqrt{\langle (\Delta I_1)^2 \rangle \langle (\Delta I_2)^2 \rangle}} = \frac{\langle \Delta I_1 \, \Delta I_2 \rangle}{\langle I_1 \rangle \langle I_2 \rangle} = \frac{|\langle \psi_1 \psi_2^{\star} \rangle|^2}{\langle |\psi_1|^2 \rangle \langle |\psi_2|^2 \rangle} = |\Gamma|^2 \tag{21}$$

The normalized covariance of intensity fluctuations is equal to the

squared modulus of the degree of coherence.

Therefore Zernike's theorem also applies to intensity fluctuations under the following form

$$\frac{\langle \Delta I_1 \, \Delta I_2 \rangle}{\sqrt{\langle (\Delta I_1)^2 \rangle \langle (\Delta I_2)^2 \rangle}} = \left| \frac{\hat{J}(\vec{a}/\lambda)}{\hat{J}(0)} \right|^2 \qquad (22)$$

The normalized spatial covariance of intensity fluctuations is given by the squared modulus of the normalized Fourier transform of the intensity distribution in the incoherent source. The measurement of this covariance is called 'intensity interferometry" by analogy with usual or amplitude interferometry.

The intensity fluctuations we have described are often referred to as thermal noise. In this classical description we have not taken into account quantum effects and the related quantum or photon noise. We shall say a word on it in part VI.

Since they are extremely rapid, thermal fluctuations are difficult to visualize. Photon noise is usually dominant in the visible range and at shorter wavelengths, whilst in the infrared or at longer wavelengths thermal noise dominates.

However the spatial properties of thermal intensity fluctuations can be easily simulated by putting a diffuser across a coherent beam of light, such as a laser beam. At some distance of the diffuser, the field is produced by superposition of a large number of statistically independant scattered beams, so that its complex amplitude obeys Gaussian statistics. The related intensity fluctuations are easily visible and called "speckle". Our mathematical description of thermal noise as well as Zernike's theorem applies equally to laser speckles.

A speckle pattern is an interference pattern. It can be considered as a superposition of interference fringes produced by any pair of points on the diffuser. Each Fourier component of the speckle noise therefore corresponds to pairs of points on the diffuser with a given spacing. The whole Fourier spectrum is given by the autocorrelation of the intensity distribution J on the diffuser, as shown by taking the Fourier transform of equation (22). The spatial correlation scale, or "speckle size", is proportional

to the inverse of the width of the illuminated part of the diffuser.

Thermal noise can also be considered as an interference pattern, but in this case the phase relationships are random so that the life time of thermal speckles is very short, being equal to the life time of the random phase relations, i.e. the coherence time τ of the light beam.

IV/ - APPLICATIONS TO ASTRONOMY

In astronomical observations, the ultimate angular resolution is limited by the diameter d of the telescope. The smaller detectable angular separation of a double star is

$$\alpha \simeq \lambda/d \qquad (23)$$

By observing interference fringes between two telescopes at a distance a apart, information is obtained on much smaller details. It is equivalent to the Young fringes experiment described above. The fringe visibility is given by the normalized Fourier transform of the intensity distribution in the object (equation 14). For a double star the visibility is a cosine function of a. The first minimum occur at a distance a, when the angular spacing of the double star is

$$\alpha = \lambda/a \qquad (24)$$

an expression similar to equation (23), but in which a can be much larger than d.

The method is very powerful for measuring the angular size α of small objects. Again the fringe visibility goes down to zero at a distance a approximately related to α by equation (24).

Michelson and his coworkers were the first to successfully apply this technique, in 1920, to the measurement of stellar angular diameters. The major problem encountered is mechanical stability (the two optical path must stay equal to within a few microns). For this reason their baseline remained limited to 12 metres. Only a few close giant stars have been measured and their technique was subsequently discarded.

A similar technique was then extensively applied by radio-astronomers. Because of the much longer wavelength there was a need

for very long baseline, in order to get the same resolution as in the visible. The mechanical stability was no longer crucial and large arrays of antennas have been built in order to map the Fourier transform $\hat{J}(\vec{a}/\lambda)$ of the intensity distribution in the object. Synthetic images have been obtained by computing the inverse Fourier transform (the technique is now called aperture synthesis).

In order to transmit signals more easily over kilometers, several techniques have been developed to reduce the signal frequency : Instead of correlating the signals from the antennas, radioastronomers correlate beats between each signal and a reference wave. This is heterodyning. It is now done over baselines as large as the earth's diameter. Another technique consists in correlating thermal noise as described above (part III). This is intensity interferometry. Thermal noise can be considered as natural beats between the different components of the signal itself.

In 1956 a radioastronomer, Handbury Brown and an opticist Twiss, suggested that intensity interferometry might work at optical wavelengths. That would solve the mechanical stability problem by correlating intensity fluctuations in the gigahertz range instead of optical frequencies. Tolerances become of the order of a few centimetres. However the normalized covariance is reduced by the ratio of the electronic to optical bandwidth.

They built large multimirrors light collectors (diameter : 6 m) and succeeded in measuring diameters of about 30 very bright stars with baselines up to 200 metres. The main drawback of this method is its very low sensitivity, which is due to photon noise. We shall come back later on this problem. Photon coincidence techniques were used to measure the correlation. The magnitude of the faintest star measured was 2.5 and the measurement required 100 hours of integration. A major advantage of this technique is its insensitivity to atmospheric turbulence which affects Michelson type interferometry. These effects will be discussed in part V.

Heterodyning is now also used in infrared interferometry by two groups : one directed by Townes in the U.S. and the other by Gay in France. However this technique also suffers from a lack of sensitivity because the bandwidth is again limited by electronics. Moreover it is sensitive to atmospheric turbulence.

Due to the work of a French opticist A. Labeyrie, there is now a considerable renewal of interest in Michelson type interferometry.

The mechanical stability problem has been solved by using concrete telescope mounting, and a small prototype instrument is already operating at C.E.R.G.A., near Grasse (France), with a baseline of the order of 20 metres. It will be increased to 40 metres in a near future. A larger instrument with two 1.5 metre telescopes is under construction. An original solution to the atmospheric turbulence problem has been developed by A. Labeyrie himself. The technique, called speckle interferometry, will be now examined.

V/ - ATMOSPHERIC TURBULENCE and SPECKLE INTERFEROMETRY

Atmospheric turbulence generates small scale temperature inhomogeneities. Due to the related fluctuations of the index of refraction, the earth atmosphere behaves like a diffuser. The angle of diffusion is of the order of a few arc-seconds.

In the visible range, it compares with the angular resolution of a lens of few centimeters in diameter. This means that the image of any telescope is blurred by such an amount. Large telescopes have been built because of their light-collecting capabilities. Through the atmosphere, their angular resolution is that of a small lens !

Due to this atmospheric problem, the size of the apertures of Michelson's stellar interferometer were limited to a few centimetres, so that the two superimposed stellar images were not blurred. However the optical path difference between the two beams was randomly varying causing a restless jigger of the observed fringes. The amplitude of this random fringe motion greatly exceeds the fringe spacing, so that fringes disapear when their motion is too fast for the eye. Happily, when the atmosphere is quiet enough, they remain visible to the observer.

Let us now examine what happens when using a single large aperture. An unresolved star is a spatially coherent light source. Observed through a diffuser it gives rise to a speckle pattern very similar to a laser speckle pattern. This speckle pattern can again be considered as a superposition of interference fringes produced by any pair of points on the telescope entrance pupil.

As in the Michelson experiment, these fringes hold high angular resolution information on the observed object but they move quite rapidly, so that the speckle pattern is always changing. On a few seconds photographic exposure time, speckles are entirely blurred out by their motion and all high angular resolution information is lost.

A. Labeyrie was the first to point out the information content of atmospheric speckles and their similarity with laser speckles. Indeed, the theory developed in part III, also applies to atmospheric speckles. As we have seen, the speckle size is proportional to the inverse of the width of the illuminated aperture. The covariance of the speckle pattern is given by equation (22) where $\hat{J}$ is now the average intensity distribution on the telescope entrance pupil, so that $\hat{J}(\vec{\alpha}/\lambda)^2$ is the intensity distribution on the Airy disk, that one would observe if turbulence was removed. The speckle size is therefore the size of the Airy disk.

Let us now examine what happens when observing an extended astronomical object $O(\vec{\alpha})$. As far as the optical paths in the atmosphere are similar, each point $\vec{\alpha}$ in the object gives rise to the same speckle pattern $S(\vec{\alpha}' - \vec{\alpha})$ shifted by an amount $\vec{\alpha}$ so that the resulting instantaneous illumination in the image plane is

$$I(\vec{\alpha}') = \int O(\vec{\alpha}) S(\vec{\alpha}' - \vec{\alpha}) d\vec{\alpha} \tag{25}$$

This convolution relation, usually written,

$$I(\vec{\alpha}) = O(\vec{\alpha}) \star S(\vec{\alpha}) \tag{26}$$

shows that the random process $I(\vec{\alpha})$ is obtained by a linear filtering of the random process $S(\vec{\alpha})$. The covariance of $I(\vec{\alpha})$ is therefore given by (†)

$$\langle \Delta I_1 \cdot \Delta I_2 \rangle = AC[O(\vec{\alpha})] \star \langle \Delta S_1 \cdot \Delta S_2 \rangle \tag{27}$$

Since $\langle \Delta S_1 \cdot \Delta S_2 \rangle$ is an Airy function, the object autocorrelation $AC[O(\vec{\alpha})]$ is obtained with the ultimate resolution of the telescope by statistically measuring the covariance of the irradiance in its focal plane. This is the principle of stellar speckle interferometry.

The same technique can be applied to a Michelson type stellar interferometer with large apertures. Each aperture produces a speckle pattern. When the two patterns are superimposed, fringes appear with

---

(†) We assume here, as a first approximation, that the process $S(\vec{\alpha})$ is homogeneous (spatially stationary) so that its covariance is a function of a single variable.

random shifts on speckle overlap areas. The fringe contrast is deduced from the covariance of this random fringe pattern.

VI/ - QUANTUM NOISE AND SIGNAL-TO-NOISE RATIO LIMITATIONS

Let us now consider the quantum aspect of radiation. At very low light level, individual photons are detected. Photon events occur randomly in time and space. The probability of detecting a photon on a small area around a point $\vec{r}$ during a small time interval around time t is proportional to the irradiance $I(\vec{r},t)$. When $I(\vec{r},t)$ is a constant, such a random process is called a *Poisson process*. Here, $I(\vec{r},t)$ is itself a random function. Such a process, with a random parameter $I(\vec{r},t)$, is called a *compound Poisson process*. In a compound process there are two types of fluctuations. Averages must be taken over fluctuations of both types.

In an intensity correlation experiment, the amount of noise is given by the variance of the statistical estimation of the correlation. Assuming a compound Poisson process, detailed calculations show that, in the very low light level limit, the signal-to-noise ratio is of the order of the number of photons per coherence area and coherence time (or number N_s of photons per speckle) multiplied by the square root of the number M of independant measurements

$$\text{Signal/Noise} \quad = \quad N_s \sqrt{M} \tag{28}$$

On such a basis, let us compare speckle interferometry with intensity interferometry. Assuming the same optical bandwidth (of the order of 200 Å) for both experiments, let n and n' be the related number of photons received per cm^2 and per second inside that bandwidth. For speckle interferometry

$$N_s = n\tau\sigma \tag{29}$$

where τ is the life time and σ the area of atmospheric speckles. And

$$M = T/\tau \tag{30}$$

where T is the duration of the experiment.

For intensity interferometry :

$$N'_s = n'\tau'\sigma' \tag{31}$$

where τ' is the life time of thermal speckles. In the Handbury Brown and Twiss experiment the area of the light collector is smaller that the area of thermal speckles, so that σ' must be taken as the area of the collector. Assuming the same duration T of the experiment, the number of independant measurements is

$$M' = T/\tau'' \tag{32}$$

where τ'' is the correlation time, much longer that the natural coherence time of thermal speckles due to the electronic low pass filtering.

The two signal-to-noise ratio are identical if :

$$n\tau\sigma\sqrt{\frac{T}{\tau}} = n'\tau'\sigma'\sqrt{\frac{T}{\tau''}} \tag{33}$$

or

$$\frac{n'}{n} = \frac{\tau\,\sigma}{\tau'\sigma'}\sqrt{\frac{\tau''}{\tau}} = \frac{\sigma}{\sigma'}\,\frac{\sqrt{\tau\tau''}}{\tau'} \tag{34}$$

With $\sigma = 10^{-3}\,m^2$, $\sigma' = 30\ m^2$, $\tau = 2 \times 10^{-2}\,s$, $\tau' = 10^{-14}\,s$ and $\tau'' = 10^{-9}\,s$, one gets :

$$\frac{n'}{n} \simeq 2 \times 10^4 \tag{35}$$

showing that intensity interferometry needs 2×10^4 times more photons than speckle interferometry in order to get the same signal-to-noise ratio. In other terms, the limiting magnitude difference between the two techniques is of the order of 11. Indeed, the limiting magnitude in the Handbury Brown experiment is 2.5 while it is of the order of 13.5 in a stellar speckle interferometry experiment.

Because of its low sensitivity, intensity interferometry is no longer used in optical astronomy. In a near future, speckle interferometry techniques will be applied to long base line Michelson-type interferometry allowing a similar angular resolution with a much higher sensitivity.

HOLOGRAPHY AND λ-CODING

J.P. Goedgebuer and J.Ch. Viénot

Laboratoire d'Optique, Associé au CNRS n° 214, "Holographie et Traitement Optique des Signaux", Universite de Franche Comté, 25030 Besançon cedex France

INTRODUCTION :

In the 1950's, D. Gabor solves the basic problem of recording and retrieving the phase, as well the amplitude of a wave. His purpose is to record electron waves and to reconstruct them in the visible domain, the advantage being to remove the difficulties linked to the spherical aberrations of electron lenses. An improvement of the resolution is expected in the images obtained in electron microscopy. His method [1] is based on the "in-line" superposition of a uniform background generated by a reference wave to the electron wave-front carrying the information. In fact the method pioneered by D. Gabor leads to twin images of poor quality. These major drawbacks are overcome 10 years later by E.N.Leith and J. Upatnieks who introduce the "off-axis" method of holography [2]. The reference and object waves impinge the holographic plate at an angle, to form very fine interference fringes. The resulting hologram acts as a grating and generates non-overlapping orders of diffraction. Each 1st order term of diffraction produces an image, and its quality is largely improved by working with diffused light. These ideas form the basis of conventional holography. A tremendous number of applications have been developed, combining the holographic process and the coherence properties of the laser sources. Before going further with conventional holography (section I), it is worth noting that a new trend has appeared for some years, by introducing white light in holography. In this case, one generally deals with wavelength-coding (section II).

I.- Conventional holography

1.- Recording and retrieving of a 3-D wavefront :

Fig. 1a represents the off-axis method of recording a hologram. Simple mathematics illustrate the reasonning. Let A_0 and A_r be the complex amplitudes of the

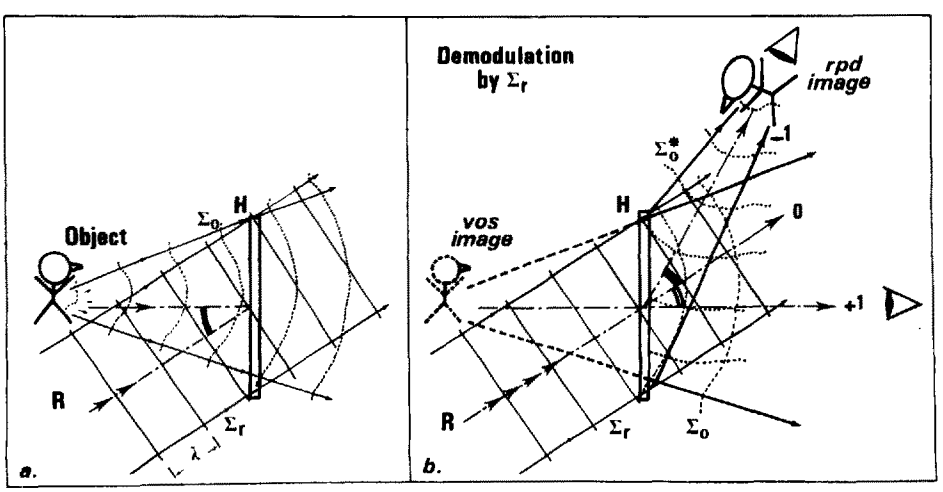

Fig. 1 : a - Recording set-up : R reference wave, O object, H : holographic plate (the dots indicate the emulsion), $\sum_0$ object wave, $\sum_r$ reference wave ;
b - Demodulation of the hologram illuminated by the reference wave $\sum_R$.

object wave and reference wave respectively. The energy E recorded on the plate is :

$$E = |A_o + A_r|^2 = |A_o|^2 + |A_r|^2 + A_r A_o^* + A_o A_r^* \qquad (1)$$

where * stands for a conjugate. This hologram is recorded under the conditions of linearity between the incident energy E and the transparency in amplitude H of the plate.

Fig. 1b illustrates the demodulation of the hologram illuminated with the reference wave. The amplitude of the light transmitted through the hologram is nothing but :

$$Ar.H = A_r(|A_o|^2 + |A_r|^2) + |A_r|^2 \cdot A_o + A_r^2 \cdot A_o^* \qquad (2)$$

Two images corresponding to the last terms of eq. (2) are reconstructed. One of them is viewed in the direction of A_0 : it is a *virtual, orthoscopic and stigmatic* image (vos) identical in position and in size to the object. The other one is generated by the second term of diffraction in the direction symmetrical of A_0 with respect to A_r. This image is *pseudoscopic* and *distorded* (p d) and thus is usually of less interest.

From a general point of fiew, the conditions of geometry or/and wavelength of retrieving may be quite different from those of recording. Object, image, size and positions are no more similar and magnification effects may occur [3,4]. As an illustration, let us consider a conjugate beam $\sum_r^*$ illuminating the hologram discussed so far. The conjugate beam $\sum_R^*$ may be obtained by inverting the direction of propagation of $\sum_r$ (Fig. 2). Eq (2) becomes :

$$A_r^* H = A_r^*(|A_o|^2 + |A_r|^2) + A_o A_r^{*2} + |A_r|^2 A_o^* \qquad (3)$$

The last term describes a conjugate object wave A_0^*. It generates a *real, pseudoscopic* and *stigmatic* image (r, p, s). Its position and size are identical to those of the object, but its relief is inverted (as in the previous arrangement, a distorted image is also obtained).

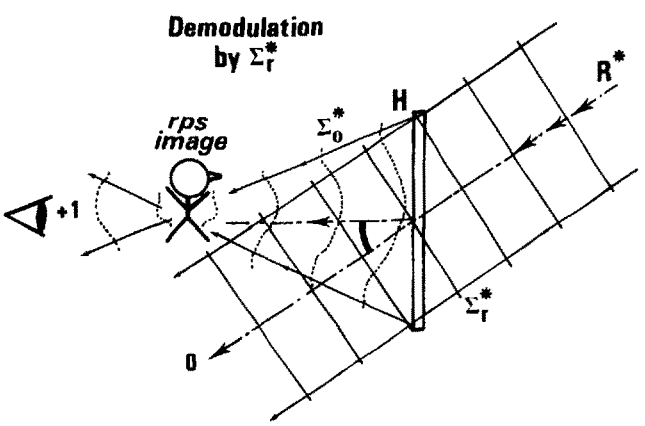

Fig. 2 : Demodulation of the hologram by a conjugate beam. A pseudoscopic image is viewed in front of the plate.

2.- Coherence requirements :

A hologram resulting from an interference phenomenon, the object and reference waves have to be spatially and temporally coherent. Practically two conditions are required when recording the hologram : (i) the two waves are emitted by a unique point source, (ii) the rays reflected from all parts of the object must interfere with the reference beam - that implies the coherence length (*) to be about twice the object depth. In general only the laser can meet this requirement, its coherence length ranging from some meters to several hundreds of meters.

One could expect that the same conditions apply to the demodulation of holograms. In fact, the demodulation requires less temporal coherence since the process does not involve any reflections, i.e. no large optical delays intervene. In these conditions, the image reconstruction can be carried out quite well with the 5461 Å line of a Hg source for instance.

II.- A cornerstone of modern holography : the introduction of white light

It would be an improvement to perform holography in white light. First, it would be advantageous in industrial and commercial applications since it would allow the hologram to be viewed anytime and any place without the use of a laser. Second, speckle effects would be smoothed, yielding a better resolution in the image.

1.- Volume Holograms [5]

The technique takes advantage of the thickness of the emulsion. The hologram is recorded in laser light. The object and reference beams are introduced from opposite sides of the plate, yielding fringes parallel to the emulsion and with a $\lambda/2$ spacing between them. When processing the plate, these fringes induce multiple reflective Ag layers ; their number may be thousands for very thick (a few mm) recording materials. The resulting hologram can be roughly described as an interference filter. Its wavelength selectivity allows the demodulation to be performed directly in white light.

2.- Rainbow holography

The recording is a two-step process based on conventional holography in laser light. The holographic images are retrieved in white light, along a λ-coding.

Fig. 3 indicates the procedure. A master hologram must be recorded first with the conventional technique (Fig. 1a). The demodulation is achieved with a conjugate beam, yielding a real, pseudoscopic and stigmatic image (r, p, s). The latter is projected through a slit and used as the object wave in the construction of a second hologram (Fig. 1b). The result is a "rainbow" hologram [6]. It can be viewed with a white light point source that illuminates the hologram at the conjugate angle of the reference beam (Fig. 1c). Each radiation of wavelength λ generates an image of the object. Each image is viewed through the corresponding reconstructed image of the slit acting as a gate. As a result, the technique provides a discrimination between the various images by displaying them individually in different colors (as a rainbow !). Unlike the volume holograms, the reconstructed image is brighter.

Last developments of this technique deal with holographic images of coloured [7] and animated [8] objects.

(*) coherence length = $1/\Delta\sigma$, where $\Delta\sigma$ is the spectral width of the source (in wavenumbers).

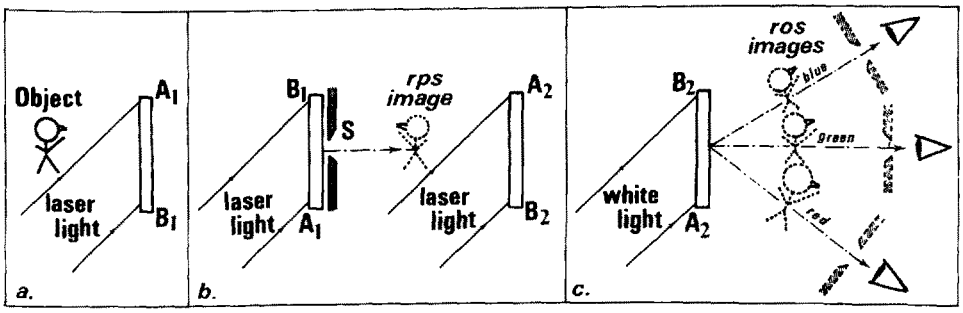

Fig. 3 : Principle of rainbow holography[6]. a - recording of a master hologram ; b - recording of a second hologram. The master hologram is illuminated by the conjugate reference beam (obtained by turning the hologram upside down) ; c - the reconstruction in white light yields polychromatic r, o, s images that are viewed through different "windows" - that prevent any color blurring.

3.- Chromatic or temporal holography

The fundamentals of holography (modulation of a spatial carrier) can be applied to the chromatic, or temporal, domain itself. It permits the recording of a so-called temporal hologram [9,10] in white light. The demodulation process is achieved in laser light. A rough idea of temporal holography can be given through the phenomenon of channelled spectrum [11]. A basic example is shown in Fig. 4. A Michelsón interferometer is illuminated by a white light point source and a spectroscope analyzes the light emerging from the interferometer. The power-spectrum $B(\sigma)$ displayed at the output of the spectroscope is [11] :

$$B(\sigma) \propto 1 + \cos 2\pi\sigma\Delta \qquad (4)$$

where Δ is the path-difference between two white light waves incident onto the spectroscope (σ : wave-number). It is a channelled spectrum. The latter can be

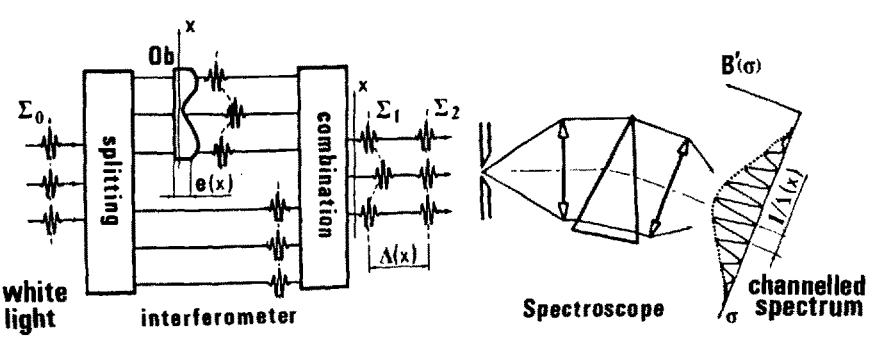

Fig. 4 : Recording of a channelled spectrum ; S white light source, Sp spectroscope. The channelled spectrum is a chromatic hologram.

considered as the superposition of the spectra of two white light waves $\sum_1$, $\sum_2$ separated by Δ, one of them playing the role of a reference with respect to the other. It comes to the description of a hologram in the temporal domain. By diffraction in monochromatic light, an "image" of the path-difference is actually reconstructed.

Unfortunately, the resolution in this type of hologram depends on that of the spectroscope and is generally low compared to that obtained with the previous methods. As a result, this method does not meet the requirements of visualization. However this technique has provided useful scientific applications, especially in metrology when measuring absolute path-differences [12]. It is why this technique is worth noting.

CONCLUSION :

A tremendous number of applications have been developed in various fields : pattern recognition, interferometry, contouring, information processing, optical memories (a volume hologram may store up to 10^9 bits/mm3), spectroscopy, optical reading, microscopy, detection of fatigue failure in materials or atmospheric pollutants, etc... Moreover the basic concepts of holography in the optical wavelengths can be generalized, and extended to other radiations (X-rays, electronwaves, acoustic waves, etc...) with applications in medicine, biology, astronomy... Some aspects of these applications are given in ref. 13.

REFERENCES :

1 - D. Gabor, Nature 161, 771 (1948)
2 - E. Leith, J. Upatnieks, J. Opt. Soc. Am. 52, 1123 (1962) ; 53, 1377 (1963) ; 54, 1295 (1965)
3 - e.g. R.J. Collier, C.B. Burckhardt, L.H. Lin, "Optical Holography" Academic Press ed., 1971
4 - e.g. J.Ch. Viénot, P. Smigielski, H. Royer, "Holographie optique ; développements; applications", Dunod ed., 1971
5 - Y.N. Denisyuck, Sov. Phys. Dokl., 7, 543 (1962) ; Opt. Spectrosc., 15, 279 (1963)
6 - S.A. Benton, J. Opt. Soc. Am. 59, 1545 A (1969)
7 - P. Hariharan, Opt. Eng., 16, 520 (1977)
8 - N. Aebischer, B. Carquille, 17, 23 (1978), 3698-3700
9 - C. Froehly, A. Lacourt, J.Ch. Viénot, Nouv. Rev. Optique, 4, 4 (1973)
10- J.Ch. Viénot, J.P. Goedgebuer, A. Lacourt, Appl. Opt., 16, 2 (1977)
11- e.g. H. Bouasse, Z. Carrière, "Interferences", Delagrave ed., Paris, 1923
12- J.P. Goedgebuer, A. Lacourt, J.Ch. Viénot, Opt. Comm. 16, 1, 99 (1976)
13- see for example "Le Courrier du CNRS", n° 28, April 1978, pp 11-19